

# In medium $T$ -matrix for nuclear matter with three-body forces - binding energy and single particle properties\*

V. Somà<sup>†</sup>

*Institute of Nuclear Physics PAN, PL-31-342 Kraków, Poland*

P. Bożek<sup>‡</sup>

*Institute of Nuclear Physics PAN,*

*PL-31-342 Kraków, Poland*

*and*

*Institute of Physics, Rzeszow University,*

*PL-35-959 Rzeszów, Poland*

(Dated: October 30, 2018)

---

<sup>†</sup> Electronic address : vittorio.soma@ifj.edu.pl

<sup>‡</sup> Electronic address : piotr.bozek@ifj.edu.pl

## Abstract

We present spectral calculations of nuclear matter properties including three-body forces. Within the in-medium  $T$ -matrix approach, implemented with the CD-Bonn and Nijmegen [1, 2] potentials plus the three-nucleon Urbana interaction [3], we compute the energy per particle in symmetric and neutron matter. The three-body forces are included via an effective density dependent two-body force in the in-medium  $T$ -matrix equations. After fine tuning the parameters of the three-body force to reproduce the phenomenological saturation point in symmetric nuclear matter, we calculate the incompressibility and the energy per particle in neutron matter. We find a soft equation of state in symmetric nuclear matter but a relatively large value of the symmetry energy. We study the influence of the three-body forces on the single-particle properties. For symmetric matter the spectral function is broadened at all momenta and all densities, while an opposite effect is found for the case of neutrons only. Noticeable modification of the spectral functions are realized only for densities above the saturation density. The modifications of the self-energy and the effective mass are not very large and appear to be strongly suppressed above the Fermi momentum.

PACS numbers: **21.30.Fe, 21.65.-f, 24.10.Cn, 26.60.Kp**

---

\*Research supported in part by the Polish Ministry of Science and Higher Education, grant N N202 1022 33

## I. INTRODUCTION

Many-body calculations based on *realistic* bare nucleon-nucleon potentials are able to reproduce qualitatively but not quantitatively the saturation properties of symmetric nuclear matter. The saturation points calculated with different approaches implemented with various choices of the nucleon-nucleon (NN) potential happen to lie on the so called Coester line in the energy per particle-density plane, away from the experimentally allowed values [4]. The theoretical predictions give a saturation density sensibly higher than the experimental value  $\rho_0 \approx 0.16 \text{ fm}^{-3}$  (usually in the range  $1.5\rho_0 - 2\rho_0$ ) and often overbind the nuclear system (up to 25%), failing to get close to the empirical binding energy  $E_0 \approx -16 \text{ MeV}$ . These discrepancies and uncertainties get amplified when calculating the equation of state (EOS) of pure neutron matter, which is necessary for the estimates of key quantities such as the symmetry energy and in general for the description of neutron-rich matter in neutron stars.

It is believed that these deficiencies originate from neglecting three-body forces (TBF) between nucleons in the dense medium. Variational and Brueckner-Hartree-Fock (BHF) calculations which take TBF into account achieve a realistic description of cold nuclear matter, reproducing the saturation point of the symmetric EOS with a good degree of accuracy [5, 6, 7, 8, 9, 10, 11, 12, 13].

The self-consistent real-time Green's functions technique can be used practically to perform calculations of in-medium propagators and properties of a many-body system. In nuclear matter this approach considers the in-medium  $T$ -matrix approximation for the two-particle Green's functions. This approximation scheme incorporates the resummation of the diagrams necessary in the presence of a strong repulsive short range component in nuclear forces and at the same time is thermodynamically consistent [14, 15]. In the zero temperature limit, the in-medium  $T$ -matrix method gives results similar to the variational and BHF approaches [16, 17, 18, 19] for the binding energy. At finite temperatures, however, it has the important advantage of automatically fulfilling the thermodynamic consistency relations, guaranteeing an unambiguous estimate of the thermodynamic quantities [15]. It has been employed in several works including studies of the modification of nucleon properties in the medium [20, 21], effective scattering [22], pairing correlations [23, 24], liquid-gas phase transition [25] and nuclear matter binding and thermodynamics [16, 18, 19, 26, 27, 28, 29, 30].

Existing self-consistent  $T$ -matrix calculations take into account only the two-body interactions, with the exception of a first attempt using a purely phenomenological Lagaris-Pandharipande TBF [31]. In the present work we implement the self consistent  $T$ -matrix scheme with two different realistic NN potentials (CD-Bonn and Nijmegen) plus Urbana three-nucleon forces, which consist in an attractive part, based on the two-pion exchange, and a repulsive term related to the presence of a Roper resonance as an intermediate state.

Within this approach we calculate the binding energy per particle for both symmetric and pure neutron matter, and give an estimate of the nuclear symmetry energy. Moreover we study the nucleon spectral function, self-energies and effective mass in comparison with the case of two-body forces only.

The paper is organized as follows. The next section is a brief review of the Green's function formalism and the  $T$ -matrix approximation. In the third section we illustrate how the three-body forces are included in the  $T$ -matrix scheme, and in section IV we present our results on the nuclear EOS and the single particle properties, placing emphasis on the modifications due to the introduction of TBF. In the last section we end with a discussion and a short summary.

At the moment we have considered the zero temperature case only. We plan to perform calculations at finite temperature, yielding thermodynamic quantities and a more complete nuclear EOS including TBF. This will be the object of a future publication.

## II. SELF-CONSISTENT $T$ -MATRIX APPROACH

In the diagrammatic expansion of the nucleon self-energy, the summation of the *ladder* diagrams at all orders leads to the  $T$ -matrix or ladder approximation [14, 32]. The imaginary part of the self-energy is obtained as follows (for more details see [30] and references therein)

$$\begin{aligned} \text{Im } \Sigma^R(\mathbf{p}, \omega) = & \int \frac{d^3k}{(2\pi)^3} \frac{d\omega'}{2\pi} \left[ \text{Im} \langle (\mathbf{p} - \mathbf{k})/2 | T^R(\mathbf{p} + \mathbf{k}, \omega + \omega') | (\mathbf{p} - \mathbf{k})/2 \rangle \right. \\ & \left. - \text{Im} \langle (\mathbf{p} - \mathbf{k})/2 | T^R(\mathbf{p} + \mathbf{k}, \omega + \omega') | (\mathbf{k} - \mathbf{p})/2 \rangle \right] \left[ b(\omega + \omega') + f(\omega') \right] A(\mathbf{k}, \omega'). \end{aligned} \quad (1)$$

Here  $b(\omega)$  and  $f(\omega)$  are respectively the Bose-Einstein and the Fermi-Dirac distributions,  $A(\mathbf{p}, \omega)$  is the nucleon spectral function related to the single particle propagator through

$$G^<(\mathbf{p}, \omega) = f(\omega) A(\mathbf{p}, \omega). \quad (2)$$

The self-consistent in-medium two-particle scattering matrix  $T$  is defined as [33]

$$\begin{aligned} \langle \mathbf{k} | T^{R(A)}(\mathbf{P}, \Omega) | \mathbf{k}' \rangle &= V(\mathbf{k}, \mathbf{k}') \\ &+ \int \frac{d^3 p}{(2\pi)^3} \frac{d^3 q}{(2\pi)^3} V(\mathbf{k}, \mathbf{p}) \langle \mathbf{p} | G_2^{nc R(A)}(\mathbf{P}, \Omega) | \mathbf{q} \rangle \langle \mathbf{q} | T^{R(A)}(\mathbf{P}, \Omega) | \mathbf{k}' \rangle, \end{aligned} \quad (3)$$

where  $V(\mathbf{k}, \mathbf{k}')$  is the chosen nucleon-nucleon potential and the uncorrelated two-particle Green's function  $G_2^{nc}$  is the product of two dressed one-body propagators

$$\begin{aligned} \langle \mathbf{k}' | G_2^{nc <(>)}(\mathbf{P}, \Omega) | \mathbf{k} \rangle &= \\ i(2\pi)^3 \delta(\mathbf{k} - \mathbf{k}') \int \frac{d\omega'}{2\pi} G^{<(>)}(\mathbf{P}/2 + \mathbf{k}, \Omega - \omega') G^{<(>)}(\mathbf{P}/2 - \mathbf{k}, \omega'). \end{aligned} \quad (4)$$

The single particle propagators are dressed via the Dyson equation

$$G^{R(A)-1}(\mathbf{p}, \omega) = \omega - \frac{p^2}{2m} - \Sigma^{R(A)}(\mathbf{p}, \omega). \quad (5)$$

Formulae (1), (3) and (5) represent a closed set of equations which has to be solved with an iterative algorithm, until self-consistency is achieved. During the iteration the Fermi energy  $\mu$  is adjusted to get the desired density  $\rho$  from

$$\rho = \int \frac{d^3 k}{(2\pi)^3} \frac{d\omega}{2\pi} G^{<}(\mathbf{p}, \omega). \quad (6)$$

Once stable solutions are obtained, the energy of the many-body system is calculated directly from the expectation value of the Hamiltonian (see [30]), avoiding the use of the Galitskii-Koltun sum rule. This is an important point because the sum rule, besides showing some dependence on the chosen energy integration cutoff, loses its validity in the presence of three-body forces.

### III. THREE-BODY FORCES

The profound reason for the appearance of three-nucleon forces is that protons and neutrons are not unstructured particles, as they are considered when constructing the various NN potentials in meson-nucleon field theory. When a nucleon interacts its internal structure indeed can be modified; this implies that there are interactions which are not anymore simply of the nucleon-nucleon type. This is usually described via the excitation of one nucleon to another state or resonance, giving rise to processes which cannot be decomposed into

a sequence of NN diagrams. At low densities their contribution is negligible, while they become relevant at densities involved in nuclear matter calculations [34].

All calculations aiming at realistic predictions of nuclear matter properties around and above the saturation point include TBF. There exist few works which implement TBF in nuclear calculations and test their effects on binding energy, pairing and single-particle properties in different approaches, both in finite systems and in nuclear matter [11, 12, 13, 35, 36, 37, 38, 39, 40].

We consider here the approach of the Urbana three-nucleon potential developed by Carlson *et al* [3]. It is composed of two terms

$$V_{ijk} = V_{ijk}^{2\pi} + V_{ijk}^R. \quad (7)$$

The first part is constructed from two-pion exchange, where a  $\Delta$  resonance appears as intermediate state. Its contribution is attractive and dominates at low densities (below nuclear saturation). The second term, whose nature is more phenomenological, provides the repulsion needed at higher densities. It is introduced to represent the contribution of several other diagrams, possibly including in an effective way also four- and more nucleon interactions. Alternative implementations and microscopic derivations of TBF are also available [34].

In more details, the Urbana TBF have the following structure

$$V_{ijk}^{2\pi} = A \sum_{cyc} \left( \{X_{ij}, X_{jk}\} \{\boldsymbol{\tau}_i \cdot \boldsymbol{\tau}_j, \boldsymbol{\tau}_j \cdot \boldsymbol{\tau}_k\} + \frac{1}{4} [X_{ij}, X_{jk}] [\boldsymbol{\tau}_i \cdot \boldsymbol{\tau}_j, \boldsymbol{\tau}_j \cdot \boldsymbol{\tau}_k] \right), \quad (8)$$

where

$$X_{ij} = Y(r_{ij}) \boldsymbol{\sigma}_i \cdot \boldsymbol{\sigma}_j + T(r_{ij}) S_{ij}, \quad (9)$$

and

$$V_{ijk}^R = U \sum_{cyc} T^2(r_{ij}) T^2(r_{jk}). \quad (10)$$

The radial functions  $Y(r)$  and  $T(r)$  are the Yukawa and tensor functions respectively, the tensor operator is defined as  $S_{ij} = 3(\boldsymbol{\sigma}_i \cdot \hat{\mathbf{r}}_{ij})(\boldsymbol{\sigma}_j \cdot \hat{\mathbf{r}}_{ij}) - \boldsymbol{\sigma}_i \cdot \boldsymbol{\sigma}_j$ , where  $\hat{\mathbf{r}}_{ij}$  is the unit vector of the distance between particles  $i$  and  $j$ . To determine the overall strength of the TBF and the relative strength between the two terms two parameters are present ( $A < 0$  and  $U > 0$ ), to be tuned to reproduce the saturation properties of symmetric nuclear matter. Since different NN potentials lead to different saturation curves one should expect these parameters to depend on the particular choice of the two-body force.

The three-body interaction depends on the spatial, spin and isospin coordinates of the three nucleons, and in such a form cannot be used in the calculations. We then need to introduce some approximation and derive an effective two-particle potential. This can be done by averaging the action of the third nucleon, resulting in a mean field felt by the other two:

$$V_{eff}^3(\mathbf{q}, \mathbf{q}') = \sum_{\sigma\tau} \int \frac{d^3k}{(2\pi)^3} n(\mathbf{k}) V^3(\mathbf{k}, \mathbf{q}, \mathbf{q}') , \quad (11)$$

where  $V^3(\mathbf{k}, \mathbf{q}, \mathbf{q}')$  is the Fourier transformed form of (7) and

$$n(\mathbf{k}) = \int \frac{d\omega}{2\pi} G^<(\mathbf{k}, \omega) \quad (12)$$

is the particle momentum distribution. The sum over spin and isospin degrees of freedom just reminds us that  $V^3$  has a non trivial structure in the  $\sigma$  and  $\tau$  spaces which has to be taken care of (we didn't write explicitly spin and isospin indices).

This average has to be performed for each of the three nucleons and over all their possible permutations, resulting in nine different terms. One has to pay particular attention to the spin-isospin and tensor dependence of the various averages and finally get, for each of the nine permutations, an effective potential of the form

$$\begin{aligned} V_{eff}^3(\mathbf{q}, \mathbf{q}') &= V_s^R(\mathbf{q}, \mathbf{q}') + V_s^{2\pi}(\mathbf{q}, \mathbf{q}') \\ &+ V_{\sigma\tau}^{2\pi}(\mathbf{q}, \mathbf{q}') \boldsymbol{\sigma} \cdot \boldsymbol{\sigma}' \boldsymbol{\tau} \cdot \boldsymbol{\tau}' + V_{S\tau}^{2\pi}(\mathbf{q}, \mathbf{q}') S(\mathbf{q}, \mathbf{q}') \boldsymbol{\tau} \cdot \boldsymbol{\tau}' , \end{aligned} \quad (13)$$

where  $V_s^R, V_s^{2\pi}, V_{\sigma\tau}^{2\pi}$  and  $V_{S\tau}^{2\pi}$  are now scalar functions.

Once we have obtained  $V_{eff}^3$  (density dependent) we add it to the two-body potential in (3)

$$V \longrightarrow V' = V + V_{eff}^3 . \quad (14)$$

and perform the  $T$ -matrix iteration.

#### IV. BINDING ENERGY AND SINGLE PARTICLE PROPERTIES

We perform calculations with two different parameterizations of the NN interaction, the CD-Bonn and the Nijmegen potentials. For both of them we compute the energy per particle directly from the expectation value of the interaction Hamiltonian, for symmetric and for pure neutron matter, with and without TBF. In the case of three-body forces we have tuned

the parameters  $A$  and  $U$  in (8) and (10) in the symmetric case in order to reproduce the saturation density  $\rho_0$  and binding energy  $E_0$ . Since the averaging over the third nucleon in TBF terms represents a rather crude approximation, the resulting numerical values of the parameters of the TBF are different than in other approaches.

### A. Symmetric nuclear matter

The energy per particle as a function of density for symmetric nuclear matter is shown in Fig. 1. The calculations with only two-body forces fail to reproduce the correct saturation behavior, predicting a saturation density  $\rho = 1.47\rho_0$  in the case of the Nijmegen potential and  $\rho = 1.79\rho_0$  for CD-Bonn. After the inclusion of three-nucleon interactions the situation is significantly improved, with both curves saturating around the phenomenological value  $\rho_0 = 0.16\text{ fm}^{-3}$  and yielding a correct binding energy [52] (Nijmegen  $E_B = -16.4\text{ MeV}$  and CD-Bonn  $E_B = -16.3\text{ MeV}$ ). We notice that the effects of TBF are almost negligible at low

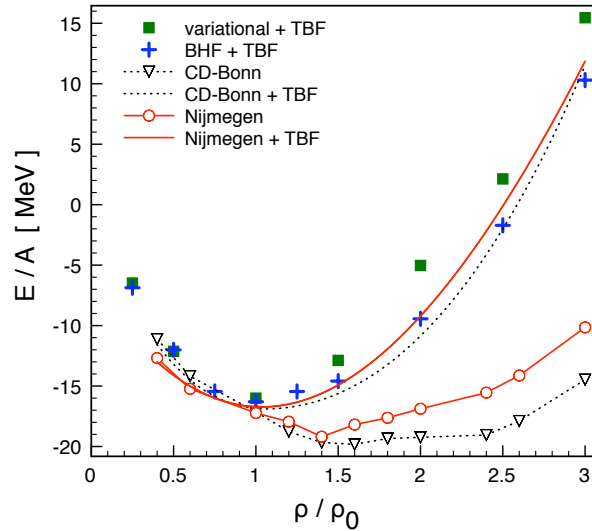


FIG. 1: (Color online) Energy per particle in symmetric nuclear matter as a function of density (in units of the nuclear saturation density  $\rho_0 = 0.16\text{ fm}^{-3}$ ).  $T$ -matrix calculations are compared to the variational [5] and BHF [13] approaches, both including TBF.

densities and become more and more significant as the density increases.

We plot for comparison also the results obtained with the variational method by Akmal et al. [5] and with the BHF approach by Baldo and Maieron [13], both using the Argonne



v18 potential. The overall agreement between all the calculations is good.

When we compute, however, the incompressibility at saturation

$$K_0 = 9 \left( \rho \frac{\partial^2 E}{\partial \rho^2} \right)_{\rho=\rho_0} \quad (15)$$

we get for both potentials  $K_0 \sim 150$  MeV, a value smaller than the usual estimates  $K_0 = 210 \pm 30$  MeV extracted from the experimental data and alternative calculation schemes.

The structure (2) of the one-particle propagator allows us to investigate the correlations induced in the dense medium by NN and three-body forces. These correlations are reflected in the energy dependence of the spectral function  $A(p, \omega)$ , which in the presence of the short-range nuclear interactions differs substantially from the  $\delta$ -function behavior that characterizes the quasiparticle approximation. In Fig. 2 we show the spectral functions when only two-body forces are present and when TBF are added for the CD-Bonn potential at three different densities and zero momentum.

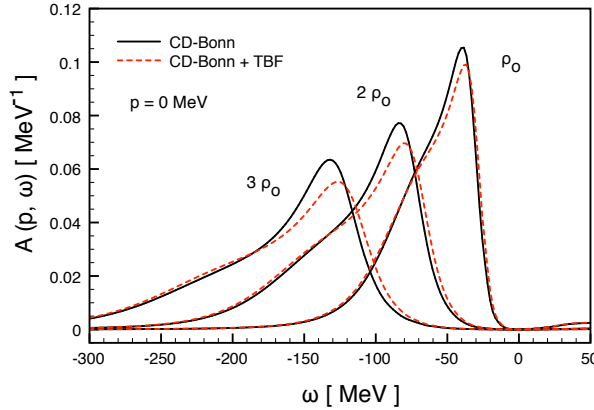


FIG. 2: (Color online) Spectral function at zero momentum for CD-Bonn interaction and symmetric nuclear matter, at  $\rho_0$ ,  $2\rho_0$  and  $3\rho_0$ .

The inclusion of TBF results in a further broadening of the peak of the spectral function, with a larger effect at high densities. This behavior reflects an increase of the scattering between the nucleons and it is common to all densities and all momenta. In Fig. 3 two cases with non-zero momenta are presented at the density  $3\rho_0$ . In the left panel ( $p$  close to the Fermi momentum  $p_F$ ), the strongest reduction of the peak shows up. The modifications caused by TBF are then slowly disappearing for higher momenta, as illustrated in the right panel. The effect of the TBF on the spectral function is minor for  $\rho < \rho_0$ . Consequently, TBF

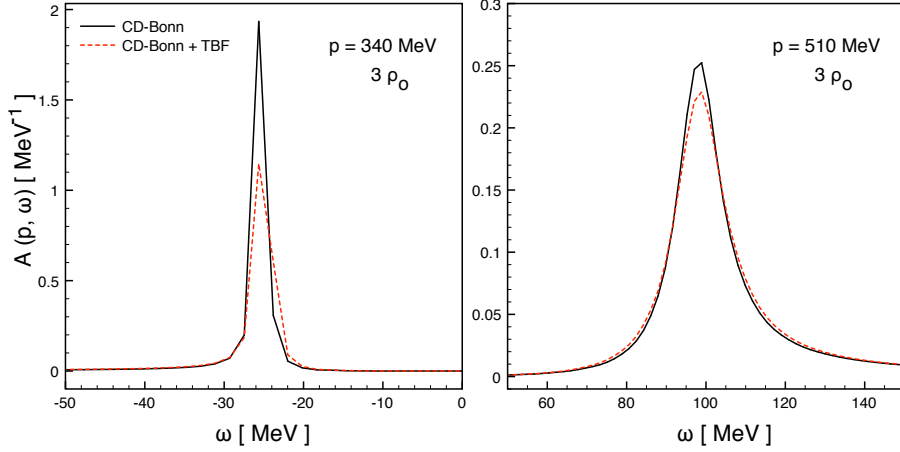


FIG. 3: (Color online) Spectral function at  $p = 340$  MeV (left panel) and  $p = 510$  MeV (right panel) for CD-Bonn interaction in symmetric nuclear matter.

and their isospin dependence cannot explain the strong dependence of the experimentally extracted proton spectral functions [41, 42, 43, 44, 45] on the target nucleus.

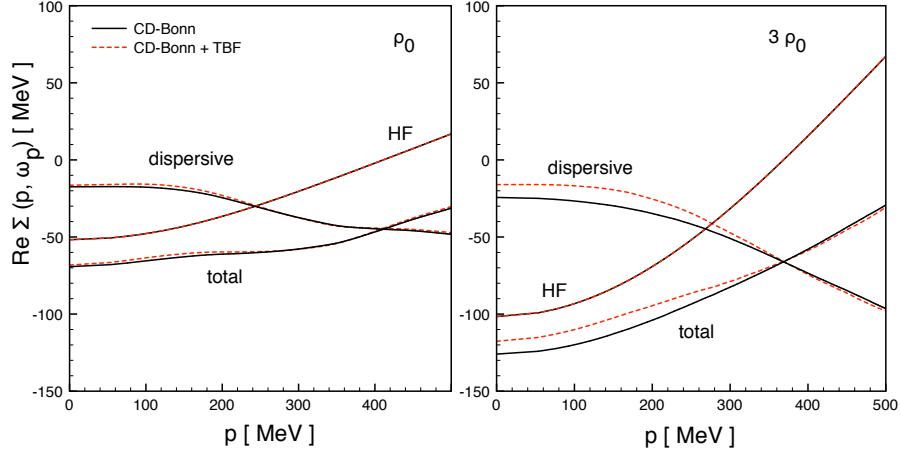


FIG. 4: (Color online) Nucleon self-energy for CD-Bonn interaction in symmetric nuclear matter at  $\rho_0$  (left panel) and  $3\rho_0$  (right panel)

We have analyzed the real part of the self-energy, which determines the shift with respect to the free dispersion relation

$$\omega_p = \frac{p^2}{2m} + \text{Re } \Sigma(\mathbf{p}, \omega_p). \quad (16)$$

It is the sum of the Hartree-Fock self-energy and a dispersive contribution obtained via the

imaginary part (1)

$$\text{Re } \Sigma(\mathbf{p}, \omega) = \Sigma_{HF}(\mathbf{p}) + \mathcal{P} \int \frac{d\omega'}{\pi} \frac{\text{Im } \Sigma^R(\mathbf{p}, \omega')}{\omega - \omega'}. \quad (17)$$

The introduction of TBF does not have a big impact on the self-energy. As shown in Fig. 4 (left panel) for low densities the modification is smaller than 5%, and it grows up to 10% at  $\rho = 3\rho_0$  (right panel). At all densities the effect is relevant for low momenta and basically vanishes above the Fermi surface. As expected TBF have a repulsive contribution, shifting the dispersive part of  $\text{Re } \Sigma(\mathbf{p}, \omega)$  up to less negative values. The behavior is completely analogous if the Nijmegen potential is employed.

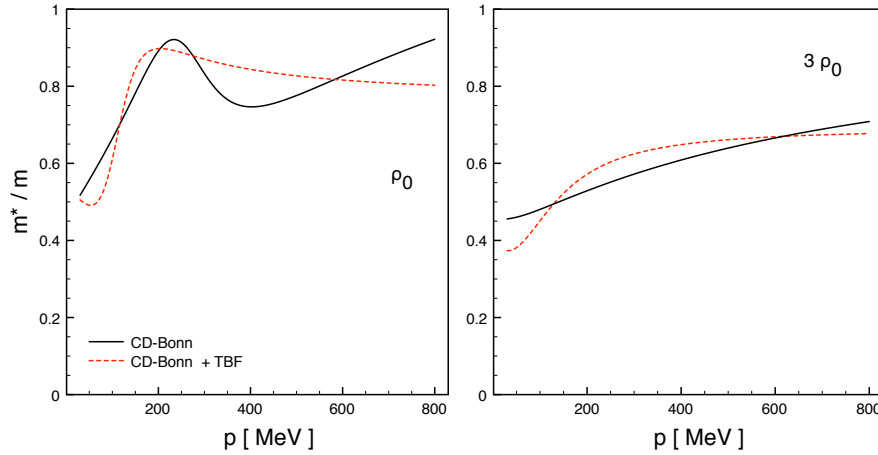


FIG. 5: (Color online) Effective mass (in units of the nucleon mass  $m = 939$  MeV) for the CD-Bonn interaction and symmetric nuclear matter at  $\rho_0$  (left panel) and  $3\rho_0$  (right panel).

Finally, the effective mass is evaluated in the presence of TBF. In general it is obtained at each momentum from

$$\frac{\partial \omega_p}{\partial p^2} = \frac{1}{2m^*}. \quad (18)$$

The effective mass as function of the momentum is displayed in Fig. 5 for the CD-Bonn potential at two different densities. As for the self-energy, the effect of the TBF is not dramatic. At  $\rho_0$  TBF smooth out the peak formed around Fermi momentum  $p_F = 263$  MeV, but do not change the value at the Fermi surface  $m^* \approx 0.85 m$  which is in agreement with the typical estimates from experiments [46] and BHF calculation with rearrangement terms included. Both with and without TBF the effective mass at  $3\rho_0$  gets substantially lower, with  $m^* \approx 0.6 m$  at the Fermi momentum. Similar behaviors are observed for the

Nijmegen NN interaction with and without three-body forces: at  $\rho_0$  we found  $m^* \approx 0.9 m$  and at  $3\rho_0$  we estimate  $m^* \approx 0.65 m$ .

## B. Neutron matter

In Fig. 6 we show the results for the energy per particle in the case of a system composed of neutrons only. For the two choices of the NN potential, curves without and with TBF are displayed. When TBF are used, the parameters  $A$  and  $U$  are fixed by the calculation in the isospin symmetric case. The introduction of TBF does not change qualitatively the density dependence of  $E/A$  but makes the EOS more stiff. As in the symmetric case the results are compared to variational and BHF calculations (both including TBF). We find agreement at low densities, with the  $T$ -matrix results getting stiffer at very high densities. A similar effect, a stiffer result from the  $T$ -matrix than from the BHF or variational calculations in neutron matter has been noticed when using two-body forces only [17].

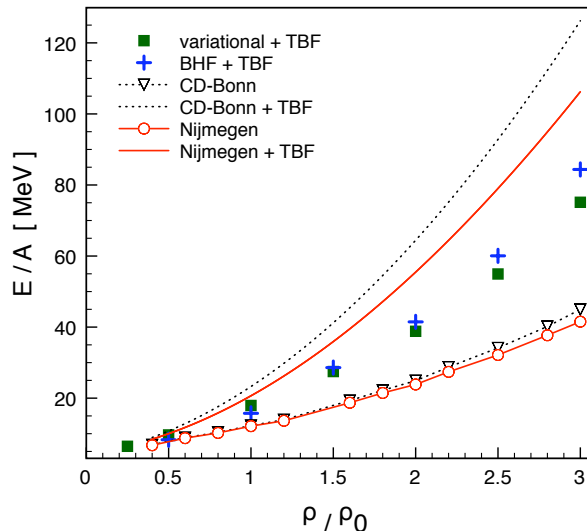


FIG. 6: (Color online) Energy per particle in neutron matter as a function of density (in units of the nuclear saturation density  $\rho_0 = 0.16 \text{ fm}^{-3}$ ) for different potentials. The  $T$ -matrix calculations are compared to the variational [5] and BHF [13] approaches, both including TBF.

An important quantity in determining the equation of state of isospin asymmetric nuclear matter is the symmetry energy. In particular its behavior is crucial for neutron star physics, since it affects the stability of neutron star matter and controls the position of the crust-core

transition [47]. The symmetry energy is defined from the energy per nucleon  $E/A$  as follows

$$E_{sym}(\rho) = \frac{1}{2} \left( \frac{\partial^2 E/A}{\partial \delta^2} \right)_{\delta=0}, \quad (19)$$

where  $\delta = (\rho_n - \rho_p)/\rho$  is the so called asymmetry parameter. We calculate  $E_{sym}$  via the parabolic approximation, which is usually employed to estimate the energy per particle for arbitrary asymmetries (whose reliability has been checked by Bombaci and Lombardo [48])

$$\frac{E}{A}(n, \delta) = \frac{E}{A}(n, \delta = 0) + \delta^2 E_{sym}(n). \quad (20)$$

The experimental measurement of the symmetry energy at saturation  $E_{sym}(\rho_0) \equiv S_0$  is not simple and still has a rather large uncertainty. A common estimate is  $S_0 = 32 \pm 6$  MeV [49]. The density dependence of the symmetry energy is of crucial importance for neutron star physics. It is fairly unknown, with large differences, specially at high densities, between the various models [50].

In Fig. 7 our result for the symmetry energy is shown in comparison with the variational and BHF approaches. When employing the CD-Bonn potential we find  $S_0 = 39.7$  MeV, for Nijmegen  $S_0 = 37.1$  MeV, both slightly higher than other estimates. With two-body forces only we find  $S_0 \simeq 30 - 32$  MeV compared to 29 MeV from an earlier self-consistent  $T$ -matrix calculation [51].

Single-particle properties in neutron matter are modified by the TBF. We present the results obtained with the CD-Bonn potential, premising that the same considerations are valid for the Nijmegen NN interaction. In Fig. 8 the spectral function at zero momentum is shown for three different densities. We see that in pure neutron matter the introduction of three-body forces causes an enhancement of the quasi-particle peak of the spectral function at all densities  $\rho > \rho_0$ . The suppression of correlations is more evident at low densities and decreases as we go up to  $3\rho_0$ .

For all momenta up to  $p_F$  there is a narrowing of the peak. The enhancement of the quasiparticle strength can be quantified as 20 – 30%. In Fig. 9 the spectral functions for two other momenta are displayed with qualitatively similar effects.

The suppression of the effects of TBF above the Fermi surface is evident when we consider the self-energy (17), plotted as a function of momentum in Fig. 10 for  $\rho = \rho_0$  (which corresponds to  $p_F = 331$  MeV) and  $\rho = 3\rho_0$  ( $p_F = 477$  MeV). The self-energy is shifted down by 5 – 10 MeV by the TBF, i.e. the single-particle potential becomes slightly more

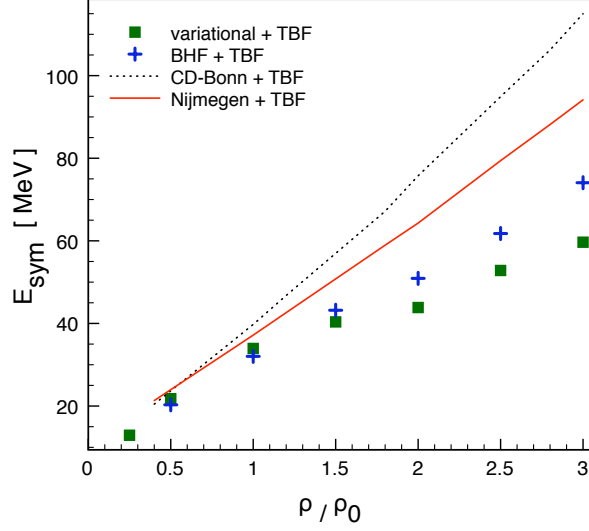


FIG. 7: (Color online) Symmetry energy as a function of the density. The  $T$ -matrix results are compared to the variational [5] and BHF [13] approaches.

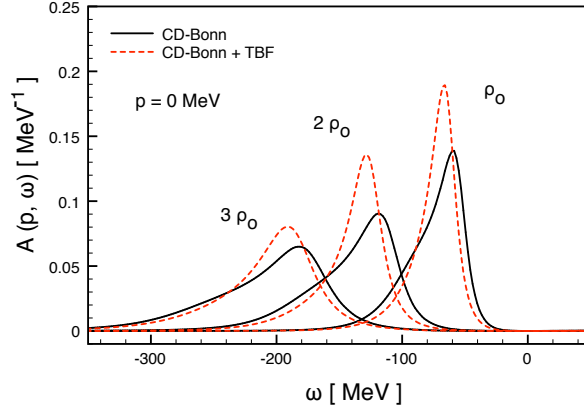


FIG. 8: (Color online) Spectral function in neutron matter at zero momentum for the CD-Bonn interaction with and without TBF.

attractive. This causes a reduction of the neutron effective mass (see Fig. 11) for momenta below  $p_F$ . Similarly to the symmetric case, for  $\rho_0$  after the introduction of TBF the structure around the Fermi momentum disappears, and the value at the Fermi surface is shifted from  $m^* \approx 0.9$  to  $m^* \approx 0.85$ . At  $3\rho_0$  there are only small differences when including TBF. With or without TBF the effective mass at the Fermi surface is found to be  $m^* \approx 0.75$ .

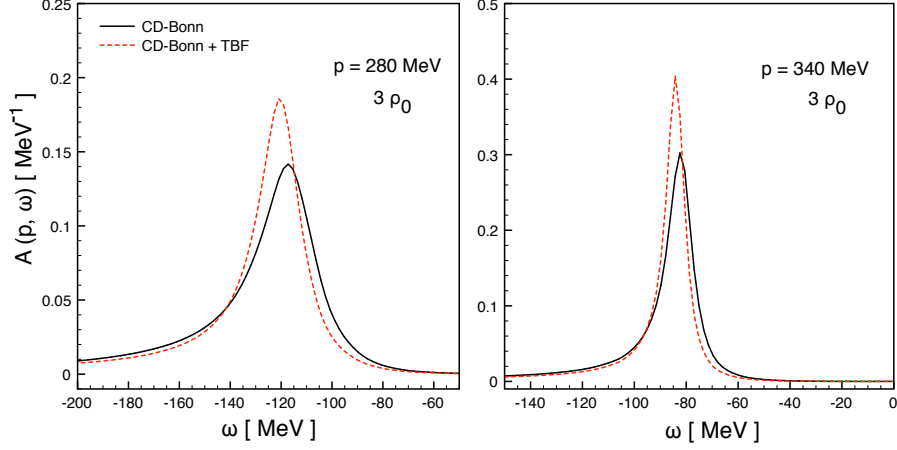


FIG. 9: (Color online) Nucleon spectral function in neutron matter at  $3\rho_0$  for  $p = 280$  MeV (left panel) and  $p = 340$  MeV (right panel).

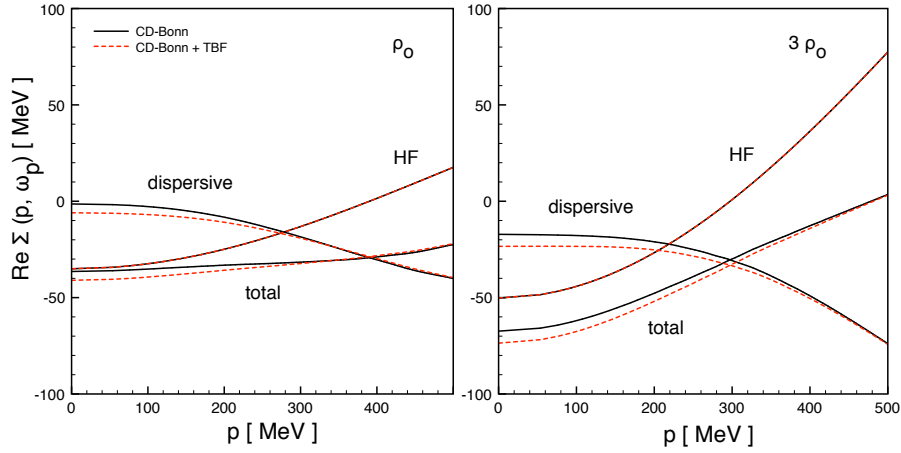


FIG. 10: (Color online) Different contributions to the self-energy  $\text{Re} \Sigma(\mathbf{p}, \omega)$  at  $\rho_0$  and  $3\rho_0$  in neutron matter (CD-Bonn interaction).

## V. SUMMARY AND CONCLUSIONS

The equation of state of symmetric and asymmetric nuclear matter is of crucial interest in the study of heavy ion collisions and the modeling of neutron stars. The self-consistent Green's function technique, in which the strong correlations induced by the nuclear interactions are resummed in the in-medium  $T$ -matrix, accounts for the modified particle properties in the dense medium and provides consistently the macroscopic thermodynamic observables.

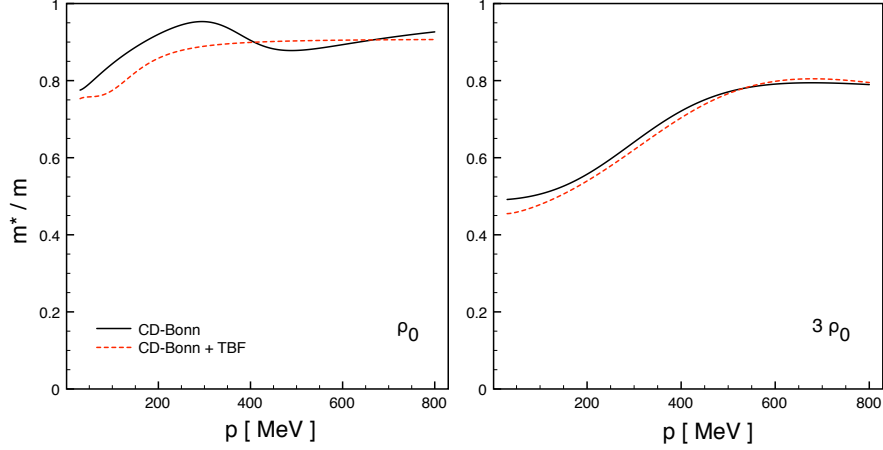


FIG. 11: (Color online) Effective mass in neutron matter (in units of the nucleon mass  $m = 939$  MeV) for the CD-Bonn interaction at  $\rho_0$  (left panel) and  $3\rho_0$  (right panel).

Within this approach, we calculate the properties of isospin symmetric and asymmetric nuclear matter at zero temperature, focusing on the impact of three-body forces on the density dependence of the energy per particle and of the single-particle properties. We employ two different NN potentials, CD-Bonn and Nijmegen, and the Urbana semi-phenomenological TBF. The results are qualitatively independent of the starting NN potential, so that the present conclusions are valid for both of them. In table I we summarize the

|                | $\rho_0$<br>[fm $^{-3}$ ] | $E_0$<br>[MeV] | $K_0$<br>[MeV] | $S_0$<br>[MeV] | $m^*/m$       |
|----------------|---------------------------|----------------|----------------|----------------|---------------|
| experiment     | $0.16 \pm 0.01$           | $-16 \pm 1$    | $210 \pm 30$   | $32 \pm 6$     | $\approx 0.8$ |
| CD-Bonn        | 0.287                     | -19.9          | 70             | 32.2           | 0.90          |
| CD-Bonn + TBF  | 0.171                     | -16.3          | 148            | 39.7           | 0.87          |
| Nijmegen       | 0.235                     | -18.4          | 76             | 30.5           | 0.87          |
| Nijmegen + TBF | 0.164                     | -16.4          | 158            | 37.1           | 0.90          |

TABLE I: Summary of the main features of the nuclear matter EOS obtained with and without TBF, compared with experimental estimates taken from [49].

most important parameters of the equation of state calculated with and without three-body forces. There is an evident improvement after the introduction of TBF, in particular in the



description of the saturation properties of symmetric nuclear matter. The incompressibility at saturation  $K_0$  is perhaps the only unsatisfactory result, being smaller than the current estimates. We have tested also a stiffer set of TBF parameters but we are not able to increase  $K_0$  without spoiling the neutron matter equation of state, which has already a stiff slope.

In general, in a dense medium three-nucleon forces play a significant role. The modifications of the EOS and of the single-particle properties are larger when the density increases. Analyzing the momentum dependence we notice that the effects of TBF are maximal around the Fermi surface, and are strongly suppressed for high momenta.

At high densities the nucleon spectral function is modified significantly. This can change the estimate of the in-medium nucleon-nucleon cross section, which is relevant for the description of heavy-ion reactions and the cooling of neutron stars. The effects depend on the isospin asymmetry of the system. It is a broadening of the quasi-particle peak of the spectral function in the case of symmetric matter, which reflects the increase of scattering between particles. On the contrary for neutron matter the peak is enhanced suggesting a stronger quasiparticle behavior. At subsaturation densities, relevant for finite nuclei, the effect of TBF on the spectral function is small. Thus, TBF cannot explain the observed strong dependence of the proton spectral functions on the average density and proton to neutron ratio in nuclei [41].

We also analyze the dispersive self-energy and the resulting optical potential is more repulsive (attractive) with TBF in symmetric (neutron) matter. The effective mass is not very sensitive to the effects of TBF. Its momentum dependence is slightly smoothed out with the introduction of TBF.

All the present results are at zero temperature. Within the  $T$ -matrix approach, it is possible to investigate the thermodynamic properties of such systems at finite temperature, including TBF forces into the calculations. TBF are a necessary ingredient in order to reach a realistic EOS of dense and hot nuclear matter.

---

[1] R. Machleidt, Phys. Rev. C **63**, 024001 (2001).

[2] V. G. Stoks, R. A. M. Klomp, M. C. M. Rentmeester, and J. J. de Swart, Phys. Rev. **C48**,

- 792 (1993).
- [3] J. Carlson, V. Pandharipande, and R. Wiringa, Nucl. Phys. **A401**, 59 (1983).
  - [4] F. Coester, S. Cohen, B. Day, and C. M. Vincent, Phys. Rev. **C1**, 769 (1970).
  - [5] A. Akmal, V. R. Pandharipande, and D. G. Ravenhall, Phys. Rev. **C58**, 1804 (1998), nucl-th/9804027.
  - [6] R. B. Wiringa, V. Fiks, and A. Fabrocini, Phys. Rev. **C38**, 1010 (1988).
  - [7] R. B. Wiringa, V. Fiks, and A. Fabrocini, Phys. Rev. C **38**, 1010 (1988).
  - [8] O. Benhar, A. Fabrocini, and S. Fantoni, Nucl. Phys. **A505**, 267 (1989).
  - [9] O. Benhar, A. Fabrocini, and S. Fantoni, Nucl. Phys. **A550**, 201 (1992).
  - [10] M. Baldo and G. F. Burgio, in *Microscopic Theory of Nuclear Equation of State and Neutron Star Structure*, edited by D. Blaschke, N. Glendenning, and A. Sedrakian (Springer, Heidelberg, 2001), vol. 578 of *Lecture Notes in Physics*, nucl-th/0012014.
  - [11] U. Lombardo and H.-J. Schulze, in *Microscopic Theory of Nuclear Equation of State and Neutron Star Structure*, edited by D. Blaschke, N. Glendenning, and A. Sedrakian (Springer, Heidelberg, 2001), vol. 578 of *Lecture Notes in Physics*, astro-ph/0012209.
  - [12] M. Baldo, ed., *Nuclear Methods and the Equation of State*, vol. 9 of *International Review of Nuclear Physics* (World Scientific, Singapore, 1999).
  - [13] M. Baldo and C. Maieron, J. Phys. **G34**, R243 (2007), nucl-th/0703004.
  - [14] L. Kadanoff and G. Baym, *Quantum Statistical Mechanics* (Bejamin, New York, 1962).
  - [15] P. Bozek and P. Czerski, Eur. Phys. J. **A11**, 271 (2001), nucl-th/0102020.
  - [16] P. Bożek and P. Czerski, Acta Phys. Polon. **B34**, 2759 (2003), nucl-th/0212035.
  - [17] P. Bożek and P. Czerski, Phys. Rev. **C66**, 027301 (2002), nucl-th/0204012.
  - [18] Y. Dewulf, W. H. Dickhoff, D. Van Neck, E. R. Stoddard, and M. Waroquier, Phys. Rev. Lett. **90**, 152501 (2003), nucl-th/0303047.
  - [19] A. Rios, A. Polls, A. Ramos, and H. Muther, Nucl. Phys. **A782**, 346 (2007).
  - [20] W. H. Dickhoff, Phys. Rev. **C58**, 2807 (1998).
  - [21] P. Bozek, Phys. Rev. **C65**, 054306 (2002), nucl-th/0201086.
  - [22] W. H. Dickhoff, C. C. Gearhart, E. P. Roth, A. Polls, and A. Ramos, Phys. Rev. **C60**, 064319 (1999).
  - [23] P. Bozek, Phys. Rev. **C65**, 034327 (2002), nucl-th/0107055.
  - [24] P. Bożek, Phys. Lett. **B551**, 93 (2002), nucl-th/0202045.

- [25] A. Rios, A. Polls, A. Ramos, and H. Muther (2008), arXiv: 0805.2318 [nucl-th].
- [26] P. Božek, Phys. Rev. **C59**, 2619 (1999), nucl-th/9811073.
- [27] Y. Dewulf, D. Van Neck, and M. Waroquier, Phys. Rev. **C65**, 054316 (2002).
- [28] P. Božek, Eur. Phys. J. **A15**, 325 (2002), nucl-th/0204034.
- [29] T. Frick and H. Muther, Phys. Rev. **C68**, 034310 (2003), nucl-th/0306009.
- [30] V. Somà and P. Božek, Phys. Rev. **C74**, 045809 (2006), nucl-th/0604030.
- [31] V. Soma and P. Bozek, Acta Phys. Polon. **B39**, 1405 (2008), arXiv: 0707.4380 [nucl-th].
- [32] J. Blaizot and G. Ripka, *Quantum Theory Of Finite Systems* (MIT Press, Cambridge, 1986).
- [33] P. Danielewicz, Annals Phys. **152**, 239 (1984).
- [34] P. Grangé, A. Lejeune, M. Martzoff, and J.-F. Mathiot, Phys. Rev. **C40**, 1040 (1989).
- [35] B. S. Pudliner, V. R. Pandharipande, J. Carlson, and R. B. Wiringa, Phys. Rev. Lett. **74**, 4396 (1995).
- [36] B. S. Pudliner, V. R. Pandharipande, J. Carlson, S. C. Pieper, and R. B. Wiringa, Phys. Rev. C **56**, 1720 (1997).
- [37] W. Zuo, A. Lejeune, U. Lombardo, and J. F. Mathiot, Eur. Phys. J. **A14**, 469 (2002), nucl-th/0202077.
- [38] X. R. Zhou, G. F. Burgio, U. Lombardo, H. J. Schulze, and W. Zuo, Phys. Rev. **C69**, 018801 (2004).
- [39] W. Zuo, A. Lejeune, U. Lombardo, and J. F. Mathiot, Nucl. Phys. **A706**, 418 (2002), nucl-th/0202076.
- [40] W. Zuo, U. Lombardo, H. J. Schulze, Z. H. Li, and J. T. U., Phys. Rev. **C74**, 014317 (2006).
- [41] D. Rohe, Eur. Phys. J. **A17**, 439 (2003).
- [42] B. Clasic et al., Phys. Rev. Lett. **99**, 242502 (2007), arXiv: 0707.1481 [nucl-ex].
- [43] P. Bozek, Phys. Lett. **B586**, 239 (2004), nucl-th/0311046.
- [44] K. S. A. Hassaneen and H. Muther, Phys. Rev. **C70**, 054308 (2004), nucl-th/0408035.
- [45] P. Konrad, H. Lenske, and U. Mosel, Nucl. Phys. **A756**, 192 (2005), nucl-th/0501007.
- [46] M. Onsi and J. M. Pearson, Phys. Rev. **C65**, 047302 (2002).
- [47] S. Kubis, Phys. Rev. **C76**, 025801 (2007), astro-ph/0611740.
- [48] I. Bombaci and U. Lombardo, Phys. Rev. **C44**, 1892 (1991).
- [49] P. Haensel, A. Y. Potekhin, and D. G. Yakovlev, *Neutron Stars 1, Equation of State and Structure* (Springer, New York, 2007).

- [50] T. Klahn et al., Phys. Rev. **C74**, 035802 (2006), nucl-th/0602038.
- [51] A. E. L. Dieperink, Y. Dewulf, D. Van Neck, M. Waroquier, and V. Rodin, Phys. Rev. C **68**, 064307 (2003).
- [52] We estimate the numerical error on all the energy calculations to be  $\pm 0.5$  MeV, for details see [30]